energies

MDPI

Article

Synthesis of Mesoporous γ-Alumina Support for Water Composite Sorbents for Low Temperature Sorption Heat Storage

Manca Ocvirk [1,2], Alenka Ristić [1,*] and Nataša Zabukovec Logar [1,3]

[1] National Institute of Chemistry, Hajdrihova 19, 1000 Ljubljana, Slovenia; manca.ocvirk@ki.si (M.O.); natasa.zabukovec@ki.si (N.Z.L.)
[2] Jožef Stefan International Postgraduate School, Jamova Cesta 39, 1000 Ljubljana, Slovenia
[3] School of Science, University of Nova Gorica, Vipavska Cesta 13, 5000 Nova Gorica, Slovenia
* Correspondence: alenka.ristic@ki.si; Tel.: +386-14760215

Abstract: The efficiency of thermochemical heat storage is crucially determined by the performance of the sorbent used, which includes a high sorption capacity and a low regeneration temperature. The thermochemical salt hydrate– γ-alumina composite sorbents are promising materials for this application but lack systematic study of the influence of γ-alumina structural properties on the final storage performance. In this study, mesoporous γ-Al_2O_3 supports were prepared by solvothermal and hydrothermal synthesis containing a block copolymer (F-127) surfactant to design thermochemical $CaCl_2$ and LiCl composite water sorbents. Altering the solvent in the synthesis has a significant effect on the structural properties of the γ-Al_2O_3 mesostructure, which was monitored by powder XRD, nitrogen physisorption, and SEM. Solvothermal synthesis led to a formation of mesoporous γ-Al_2O_3 with higher specific surface area (213 m^2/g) and pore volume (0.542 g/cm^3) than hydrothermal synthesis (147 m^2/g; 0.414 g/cm^3). The highest maximal water sorption capacity (2.87 g/g) and heat storage density (5.17 GJ/m^3) was determined for W-46-LiCl containing 15 wt% LiCl for space heating, while the best storage performance in the sense of fast kinetics of sorption, without sorption hysteresis, low desorption temperature, very good cycling stability, and energy storage density of 1.26 GJ/m^3 was achieved by W-46-$CaCl_2$.

Keywords: mesoporous γ-Al_2O_3; TCM composite; hydrothermal synthesis; structural properties; water sorption capacity; sorption heat storage

Citation: Ocvirk, M.; Ristić, A.; Zabukovec Logar, N. Synthesis of Mesoporous γ-Alumina Support for Water Composite Sorbents for Low Temperature Sorption Heat Storage. *Energies* **2021**, *14*, 7809. https://doi.org/10.3390/en14227809

Academic Editor: Elpida Piperopoulos

Received: 15 October 2021
Accepted: 19 November 2021
Published: 22 November 2021

1. Introduction

Thermochemical energy storage (TCES), as one of the three technologies of thermal energy storage (TES), can reduce fossil fuel consumption, which still dominates building space heating, by shifting some of the solar thermal energy collected in summer to winter [1]. Thermochemical heat storage uses the reversible chemical reaction (reaction of water and $CaCl_2$) and/or sorption processes of gases in solids or liquids (water sorption on porous solids). Water sorption heat storage consists of two phases. In the first phase, which is also called charging or desorption, gas or water vapour is desorbed from the material under solar radiation or waste heat. In the second phase or discharging (adsorption), the water vapour is adsorbed on the material with heat release, which can be used for space heating. The efficiency of the sorption technology, based on the alternating (ad)sorption (exothermic phenomenon) and desorption (endothermic phenomenon) of the working fluid on the sorption materials, is determined by the performance of the used sorbent, which should have a high sorption capacity, and consequently a high energy storage density, a low regeneration temperature of 80 to 120 °C, stability in humid conditions and also at temperatures up to 120 °C, and no hysteresis (of the sorption and desorption curves) during the sorption cycles. These requirements can be accomplished by the thermochemical (TCM) composite sorbents [2], formed of various porous supports and hygroscopic salt hydrates (halides, nitrates, sulphates) and are currently the most studied sorbents, especially when

water is used as the working fluid. The process of water sorption in these composites can consist of three mechanisms: adsorption of water on the active support, chemical reaction between water and entrapped salt in the pores of the support, and absorption of water in salt solution in the pores [3]. The main advantage of these sorbents is tailoring their sorption properties by changing the structural properties and chemical composition of the support, and by entrapping of the particular hygroscopic salt hydrate nanoparticles in the support.

A brief review of the literature on the composites for thermochemical energy storage has shown that the increase in sorption capacity has mainly occurred by changing the salt hydrate and increasing its amount [4]. Fewer TCES studies have been carried out on the development of the active porous support, which can be involved in the adsorption process to further improve the storage performance in the context of increased sorption capacity by adjusting the chemical composition of the support and creating additional adsorption sites by using different synthesis routes [5–8]. Porous supports for TCM composites found in the literature are mainly commercial materials such as Zeolites [9], silica gels [10], activated alumina [11], and vermiculite [12], while recently, novel supports such as MOFs [13], polymeric foam [14], alginate [15], and porous carbon structures [16–18] have been used.

An important task in the preparation of salt hydrate TCM composites is the selection of the support for the salt inclusion. The support should meet certain requirements such as the ability to provide a stable nano-environment for salt confinement, hydrothermal stability, stability of the pore structure under working conditions, inertness to salt hydrates, and good thermal conductivity, to name a few, to enhance the performance of the composite. In addition, a simple and environmentally friendly synthesis that leads to the preparation of the composite and does not show hysteresis during sorption is of great importance [19].

To date, TCM composite sorbents based on mesoporous alumina (Al_2O_3) [20,21] or activated alumina [11,22–24] have been prepared from commercially available aluminas and combined with the following salt hydrates: $MgSO_4$, LiCl, and $CaCl_2$. These alumina composites have been investigated for thermochemical heat storage at low temperature (<100 °C). Recently, anodic alumina was prepared by anodizing of aluminium sheet and used for the salt composites [25,26]. In all these studies, only the physicochemical properties of the alumina support, such as specific surface area or pore volume and pore size, were shown, and it was not evident whether crystalline or amorphous alumina was used. Indeed, aluminas exist as amorphous or crystalline phases of various oxides and oxyhydroxides. The crystalline structures, which are mainly composed of γ, δ, ρ and α phases, exhibit different properties. All these structures can be prepared by irreversible thermal transformation of the crystalline aluminium hydroxides and salts or by colloidal gel precipitation. α-Al_2O_3 is the high-temperature end product of the thermal treatment [27]. For example, the γ-Al_2O_3 support is often described as robust, thermally stable, and easy to shape. In addition, it offers acid-base properties with polarity [28], favourable surface properties, such as high specific surface area (100–400 m^2/g) and a tendency to disperse the active phase. Together with its low price, alumina is at the top of the list of the used supports in catalysis and adsorption [29]. The thermal and hydrothermal stability strongly depends on the synthetic methods and conditions.

Mesoporous alumina is most commonly obtained by sol-gel synthesis using soft or hard templates and by evaporation-induced self-assembly (EISA). Sol-gel synthesis in the presence of soft templates is one of the most common methods for preparing mesoporous alumina. The soft templates can be anionic (stearic acid, etc.), cationic (CTAB, etc.), nonionic (P123, etc.) surfactants, as well as non-surfactants (ionic liquids) [29]. The alumina precursor, usually aluminium isopropoxide, and the surfactant were dissolved in alcoholic solvent with the minimum amount of water added to promote hydrolysis of the isopropoxide and start the condensation reaction. Further evaporation of the solvent led to the formation of the ordered or disordered mesoporous inorganic substance [27,30,31]. Its final structural properties also depend significantly on the thermal treatment (e.g., calcination) during the removal of the template. Calcination is an important parameter in creating crystalline

alumina with high surface area and has a great impact on the thermal, hydrothermal, and mechanical stability of alumina. The use of higher temperatures improves the crystallinity of porous materials but has a drawback, which can be seen in reduction in their mesostructural order as well as in the reduction in their pore volume and specific surface area [32].

The aim of this study is to design γ-alumina supports with mesoporous character, to determine the influence of the synthesis route using different solvents (water/ethanol/ethanolic solution) on the textural properties of the mesoporous γ-alumina support, to combine mesoporous γ-alumina supports with LiCl and $CaCl_2$ salt hydrates, and to determine water sorption properties of these composites. In addition, the stability for the composites of the water-based γ-alumina (W-46) with $CaCl_2$ and LiCl under humid conditions up to 100 °C has been evaluated. Crystalline γ-alumina has been selected as the support for the composite due to its thermal conductivity of 30 W/mK, which can further promote heat transfer in the system compared to silicate supports with a much lower thermal conductivity of 0.2 W/mK.

To the best of the author's knowledge, this is the first report on the synthesis of crystalline mesoporous γ-alumina as a support for the TCM composite water sorbents.

2. Materials and Methods

2.1. Materials Synthesis

Pluronic F-127 ($EO_{106}PO_{70}EO_{2106}$) and aluminium isopropoxide (98%) were purchased from Aldrich. Nitric acid (67%) and absolute anhydrous ethanol (99.5%) were purchased from Sigma-Aldrich (Darmstadt, Germany) and CARLO ERBA Reagents (Milan, Italy), respectively. Calcium chloride hexahydrate (98%) and lithium chloride hydrate (99%) were purchased from Sigma Aldrich (Darmstadt, Germany).

2.1.1. The γ-Alumina Support Synthesis

Mesoporous γ-alumina samples were synthesised in a two-step procedure. First, the evaporation-induced self-assembly (EISA) method was used. The following procedure is an adaptation of the synthesis described in [31]. The molar ratio of the reactants was: 1 AIP: 0.006 F-127: 2.3 HNO_3: 68 ethanol or water and 1 AIP: 0.006 F-127: 2.3 HNO_3: 34 ethanol: 34 water.

In all syntheses, two solutions were prepared: *solution A* containing solvent (an ethanol or a water or an ethanolic solution) and aluminium isopropoxide (AIP), and *solution B* containing a triblock copolymer non-ionic surfactant F-127, the same solvent as in solution A and nitric acid to aid solubility and hydrolysis.

Both types of solutions (*A* and *B*) were stirred at room temperature until completely dissolved and then mixed together and stirred at room temperature for 5 h. After solvent evaporation at 60 °C for 48 h in an oven, a semi-transparent solid was obtained. In the second step, the obtained solids were further solvothermally (ethanol) or hydrothermally (water, ethanolic solution) treated in Teflon-lined stainless steel autoclaves at 160 °C for 12 h.

The as-prepared samples were calcined in the furnace at 800 °C for 3 h under air flow with a temperature ramp of 1.6 °C/min to remove the surfactant and achieve the transformation of the precursor phase to crystalline γ-alumina.

The prepared support samples were named after the solvent used: water (W-46), ethanol (E-37), and ethanolic solution (ES-47).

2.1.2. Composite Preparation

The mesoporous γ-Al_2O_3 prepared with water and ethanolic solution was preheated in the oven at 120 °C for 2 h. A predetermined quantity of $CaCl_2 \cdot 2H_2O$ and $LiCl \cdot H_2O$ was dissolved in 1 mL of deionized water in order to reach the required salt amount. The prepared salt solutions were then spread to the dehydrated mesoporous γ-Al_2O_3 using

the incipient wetness impregnation method. The composites were dried over night at room temperature.

2.2. Methods

XRPD patterns were collected on a PANalytical X'Pert PRO high-resolution diffractometer (Almelo, The Netherlands) from 10 to 70° 2θ, and a fully opened X'Celerator detector.

Nitrogen physisorption was performed at 77 K on a Tristar3020 volumetric analyzer (Micromeritics, Norcross, GA, USA). The nonporous salt does not contribute to nitrogen adsorption to a large extent, so the amount of the salt was considered, and nitrogen isotherms, specific surface area, and pore volume values were corrected. The BET specific surface area was calculated from adsorption data ranging from 0.05 to 0.2 of relative pressure [33]. The total pore volume was evaluated at a relative pressure of 0.98. The KJS method [34] was used to determine the pore size distribution (PSD), and the maximum of the PSD was used for the pore diameter determination [35].

SEM images were recorded on Verios 4G HP field-emission gun microscope (Thermo Fisher Scientific, Waltham, MA, USA).

Energy dispersive X-ray analysis (EDAX) using Zeiss SupraTM 3VP microscope (Jena, Germany) and ICP-OES using spectrometer ES 715 (Varian, Palo Alto, Santa Clara, CA, USA) were performed for elemental analysis.

The desorption temperatures of W-46 and ES-47 composites were determined using a Q5000IR thermogravimetric analyser (the accuracy ±0.01 μg; ±0.1 °C) (TA Instruments, Inc., New Castle, DE, USA) where the maximum (Tpeak) of the DTG curve was considered the desorption temperature [36]. The samples were heated in air at a heating rate of 10 °C/min. Before thermogravimetric measurements, the samples were kept over a saturated potassium sulphate solution for 5 days.

The surface charge of the W-46 and ES-47 supports was measured using Zetasizer nano ZS (Malvern, UK) instrument.

Water sorption isotherms were measured using the IGA-100 gravimetric analyser (the accuracy ±0.1 μg) (Hiden Isochema Ltd., Warrington, UK) at 25 and 35 °C and used to the calculate the value of the differential enthalpy of sorption according to the well-known Clausius–Clapeyron equation. The equal pressure intervals of 1.6 mbar between vacuum and 40 mbar (saturation vapor pressure of 56.3 mbar) were set with an equilibrium time of 80 s. The samples were degassed at $<10^{-5}$ mbar at 25 °C (the accuracy ±0.1 °C) for 4 h to a constant mass. The definition of the thermodynamic heat cycle is shown in [37], and the calculation of the amount of heat involved can be found in [38]. The integral enthalpy of sorption Q_{sor} can be considered as the achievable heat storage density at the material level and was calculated by using the following equation: $Q_{sor} = \Delta H_{sor} (w_{sor} - w_{des})$ [kJ/kg_{sor}]. ΔH_{sor} [kJ/kg_{water}] is the differential enthalpy of sorption according to the sorbed water amount, and w_{sor} and w_{des} [kg_{water}/kg_{sor}] are the maximum and minimum sorbed water amount over the sorbent at the given boundary conditions. The specific heat of the γ-alumina is 94.6 kJ/mol K at 25 °C [39]. The integral heat of sorption was calculated for the application of heat storage.

The sorption/desorption cycling performance [38] of the W-46-$CaCl_2$ and W-46-LiCl composites were carried out on IGAsorp-XT automated water sorption gravimetrical analyser (the accuracy ±0.1 μg) (Hiden Isochema Ltd., Warrington, UK.) with the sequential procedure of water uptake measurements at 35 °C (the accuracy ±0.1 °C) under moist nitrogen gas flow (flow rate of 250 mL/min and 80% relative humidity) for 3 h, followed by drying at 100 °C with dry nitrogen flow for 2 h. The sequence was repeated 25 times according to the literature [40] at a desorption temperature of 100 °C, which can be attained by solar thermal collectors. The sorption temperature was fixed to 35 °C, which is sufficient for space heating applications. The water vapor pressure during desorption and sorption of the samples was set to 12.3 mbar (a dew point temperature of 10 °C). The difference in the amount of sorbed water at 35 °C and 100 °C at 12.5 mbar is the cycle (water) loading lift of the composite.

3. Results and Discussion

3.1. Structural Properties of All γ-Alumina Supports and Composites

All mesoporous γ-alumina supports were prepared by the same synthesis procedure, which differs only in the use of different solvents (i.e., ethanol, water, and ethanolic solution), while the other conditions remained the same. The calcined samples exhibited mesostructures of all γ-alumina with low crystallinity, which can be due to the high calcination temperature (800 °C) [29] after the second step of hydrothermal or solvothermal treatment. Grant et al. [31] obtained cage-like ordered mesoporous γ-alumina by one-step synthesis, i.e., evaporation-induced self-assembly synthesis and calcination at 400 °C. Powder XRD was used to identify the crystal structure of the products after thermal treatment at 800 °C. The calcined powders in Figure 1a exhibited diffraction peaks corresponding to the γ-Al_2O_3 phase, which is consistent with JCPDS 00-050-0741. It can be observed that the intensity of the characteristic peak at 2θ 66.5° decreases in the sample prepared by hydrothermal synthesis compared to the sample prepared by solvothermal synthesis, indicating higher crystallinity of the solvothermal product. All the diffraction peaks are quite broad, which can be due to nanosized particles of the γ-Al_2O_3 products. The diffraction peak at 2θ 44.2° in the W-46 sample belongs to the XRD sample holder.

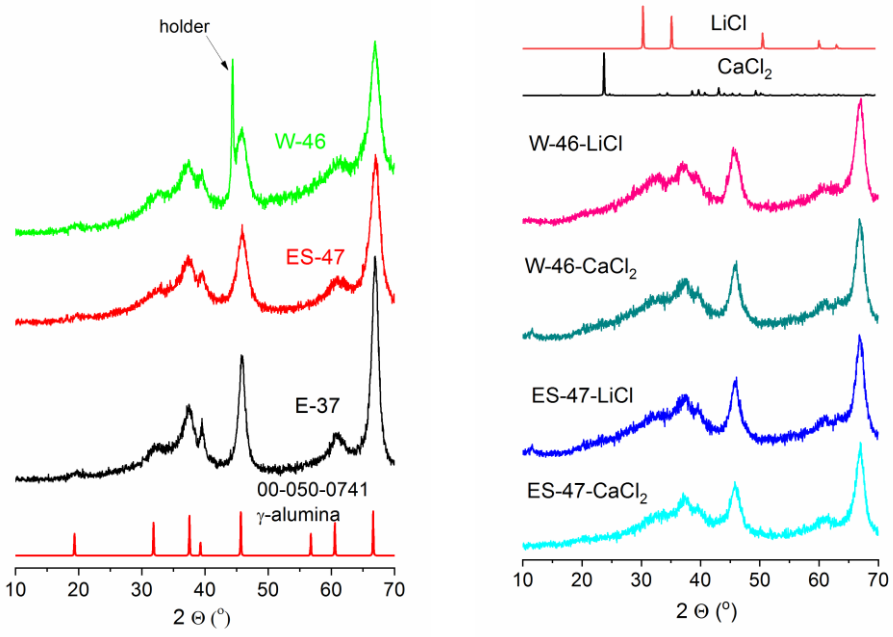

Figure 1. Powder XRD patterns of (**a**) γ-Al_2O_3 products obtained after thermal treatment at 800 °C and (**b**) $CaCl_2$ and LiCl composites with W-46 and ES-47 γ-Al_2O_3 supports.

γ-Al_2O_3 supports prepared from water (W-46) and ethanolic solution (ES-47) were used to prepare the composites, as their crystal structure was preserved after treatment at 100 °C for 5 h in vacuum. Introduction of $CaCl_2$ and LiCl salts into mesoporous γ-Al_2O_3 prepared in water and ethanolic solution revealed that the supports were inert to the salts, meaning that the crystal structure of the supports did not change or react with these salts (Figure 1b). Additional peaks due to the presence of the salts were not observed, indicating that the highly dispersed salts were successfully confined of in the mesopores of these supports and/or that the salts were dispersed in particles less than 5 nm in size, which are not detected by XRD.

The morphology of the hydrothermally prepared γ-Al_2O_3 supports (E-37, W-46, and ES-47) was investigated using SEM (Figure 2). The results showed that the particular solvent used in the synthesis had a significant effect on the morphology of the samples. In

water, larger 3 μm γ-Al_2O_3 agglomerates were formed, while 100 nm and 25–50 nm round nanoparticles were obtained from the ethanol and ethanolic solution-containing, respectively.

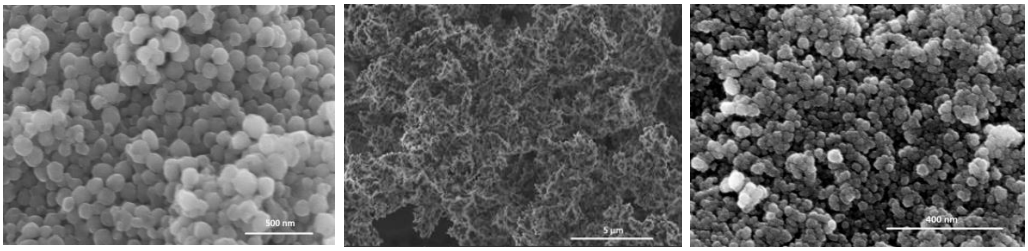

(**a**) (**b**) (**c**)

Figure 2. SEM pictures of hydrothermally prepared mesoporous γ-Al_2O_3 supports: (**a**) E-37, (**b**) W-46, and (**c**) ES-47.

The amount of impregnated $CaCl_2$ after the incipient wetness impregnation procedure on W-46 and ES-47 γ-Al_2O_3 supports was lower than expected, considering the amounts of inorganic salt used in the composites with silica [8]. This is reported to be influenced by the high polarity of the alumina [28] and pH. The dependence of surface charge of γ-alumina (W-46 and ES-47) on pH is illustrated in Figure 3. It can be seen that the solvents affect the surface charge of the prepared supports. At the pH value of $CaCl_2$ and the LiCl solutions (pH = 5.5), the W-46 γ-alumina support exhibits a positively charged surface (29 mV), as does the ES-47 γ-alumina support (28 mV).

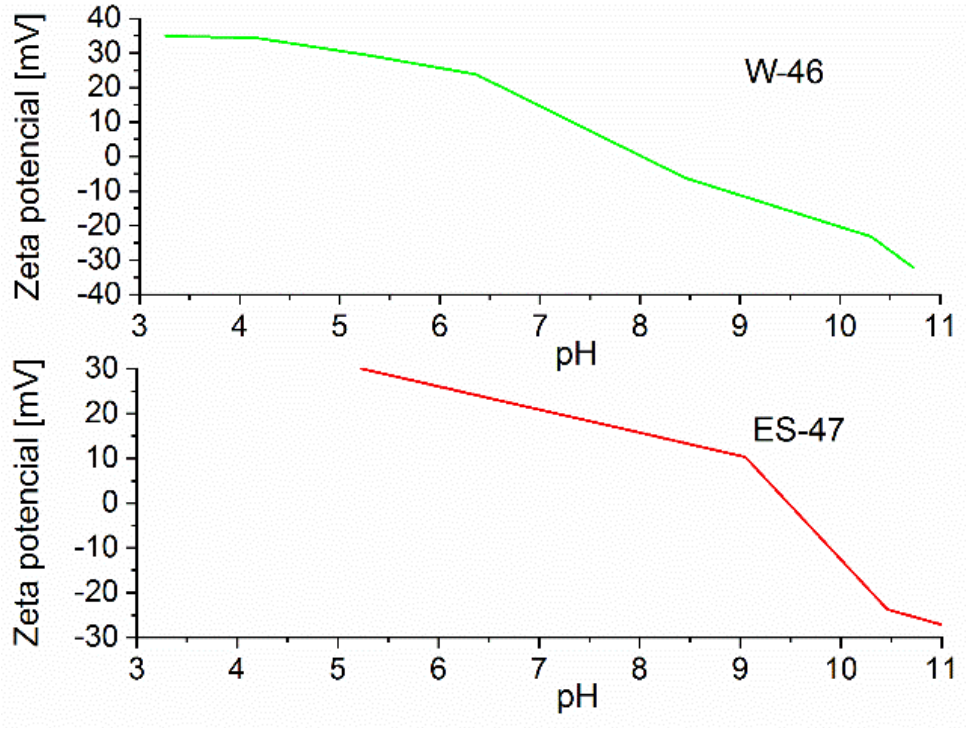

Figure 3. Surface charge of γ-alumina supports W-46 and ES-47.

Thus, the introduction of calcium chloride or lithium chloride solution into the mesopores of the W-46 or ES-47 support during incipient wetness impregantion was hindered by similarly charged species, compared to silica mesostructures with negatively charged surface (−20 mV) [41]. The negatively charged surface (−10 mV) of the γ-alumina support W-46 can be obtained at a lower pH than ES-47. In general, the surface charge can be changed by modifying the synthesis procedure.

EDX analysis determined 10 wt% $CaCl_2$ in both supports, while determination of LiCl was performed using ICP-OES. In the W-46 and ES-47 supports, 15 wt% and 10 wt% LiCl were determined, respectively.

Nitrogen physisorption measurements were used to evaluate the textural properties of γ-Al_2O_3 supports prepared from different solvents. The nitrogen adsorption isotherms of the γ-Al_2O_3 supports and their pore size distributions (PSDs) are shown in Figure 4a, the composites W-46 in Figure 4b, and the composites of ES-47 in Figure 4c. The textural parameters determined based on these isotherms are listed in Tables 1 and 2. All isotherms are of Type IV, which is typical of mesoporous materials [42]. The isotherms exhibit a capillary condensation step, indicating the presence of mesoporosity. The sample E-37 shows a steeper capillary condensation, which is typical of a narrow pore size distribution. It can be clearly seen that the hysteresis loops change from the H1 loop for samples E-37 and ES-47 to the H3 loop for W-46, indicating different γ-Al_2O_3 support mesostructures due to the solvent used. The H3 loop is typical of materials with slit-like mesopores [42]. Macroporosity is found in the W-46 sample (Figure 4a) but not in the ES-47 and E-37 samples. The capillary condensation step for the ES-47 sample is shifted towards higher relative pressures, indicating an increase in the size of the mesopores due to solvothermal synthesis [43].

The E-37 sample has the highest specific surface area and pore volume (Table 1), while samples ES-47 and W-46 have lower specific surface areas and pore volumes. The largest size of mesopores (11.3 nm) was determined from the maximum of pore size distribution (Figure 4a), for sample, ES-47 prepared from ethanolic solution. On the other hand, the smallest size of mesopores (9.1 nm) was determined for the W-46 sample prepared hydrothermally.

The inclusion of salts in both supports resulted in less intense hysteresis loops (Figure 4b,c) and pore size distributions (Figure 4b,c), accompanied by a decrease in pore sizes, pore volumes, and specific surface areas (Table 2). It can be concluded that the salt nanoparticles been dispersed inside of mesopores of the supports. For example, after the introduction of LiCl into the W-46 support, the specific surface area (68 m^2/g) and pore volume (0.196 cm^3/g) of the composite decreased significantly (Table 2). The pore diameter (8.7 nm) of this composite was larger than the pore diameter (8.3 nm) of the composite with $CaCl_2$.

Desorption temperatures for the composites were determined from the DTG curves for composites W-46 and ES-47, which are shown in Figure 5. The desorption temperature of water was completed for the W-46 samples in the following order: the W-46-$CaCl_2$ sample (98 °C), the W-46-LiCl (88 °C), and the W-46 support (29 °C) (Figure 5a). Additionally, 88.0% of the water was desorbed from the composite containing LiCl, while a smaller amount of water (74.9%) was removed from the composite containing $CaCl_2$. The DTG curves show one water loss for all samples prepared in water and ethanolic solution. Water can be removed from W-46 composites at 120 °C. For ES-47 composites, water desorption can be completed even at a lower temperature (100 °C). Desorption temperature for the ES-47-LiCl composite was 68 °C, while a slightly lower desorption temperature (62 °C) was observed for ES-47-$CaCl_2$ (Figure 5b). Additionally, 75.0% and 60.8% of water was removed from the ES-47-LiCl and ES-47-$CaCl_2$ composites, respectively.

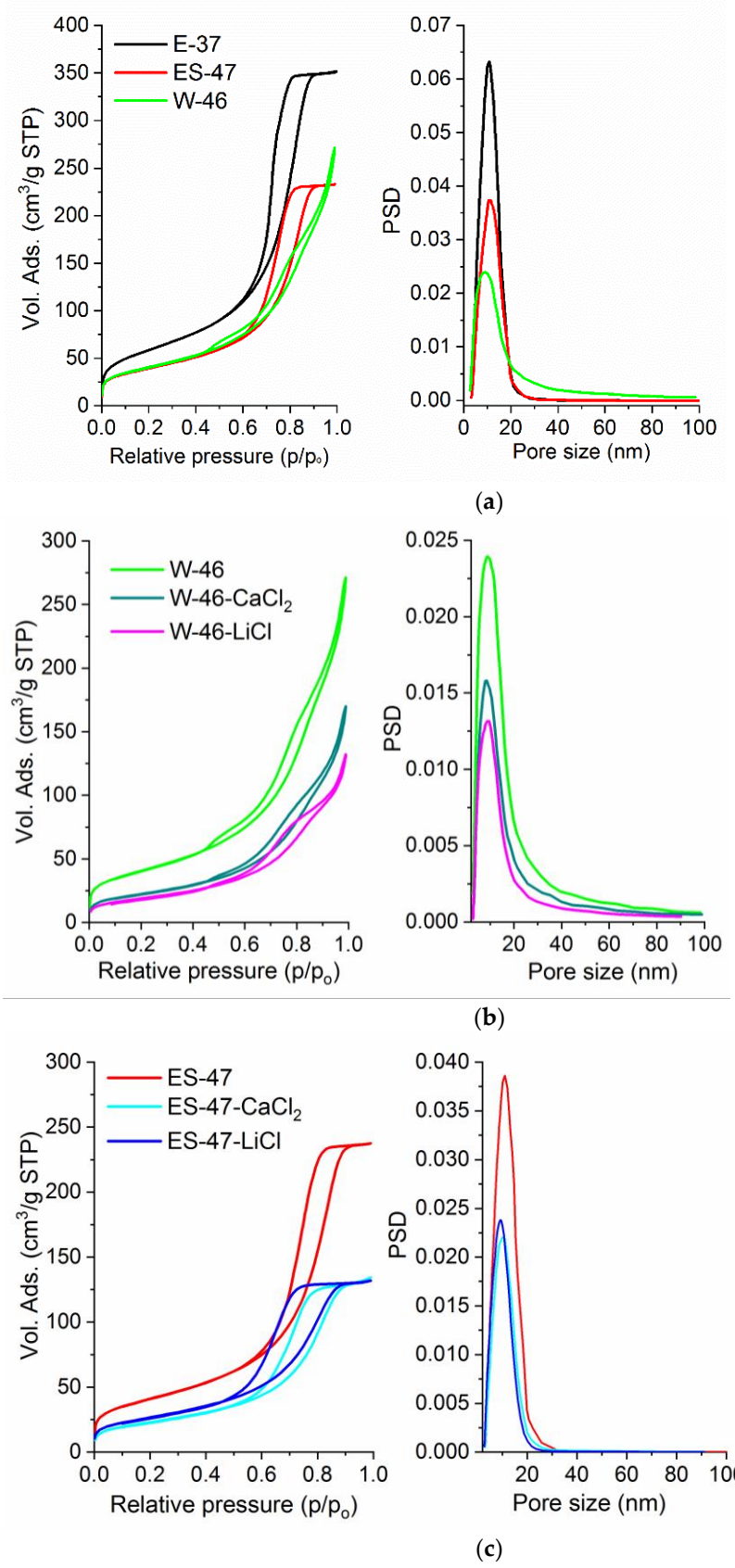

Figure 4. Nitrogen sorption isotherms of (**a**) γ-alumina supports with corresponding PSDs, (**b**) W-46 and its composites with corresponding PSDs, (**c**) ES-47 and its composites with corresponding PSDs.

Table 1. Textural properties of the mesoporous γ-Al_2O_3 supports.

Sample Support	Solvent	S_{BET} (m^2/g)	Vp (cm^3/g)	Average Pore Size (nm)
E-37-γ-Al_2O_3	Ethanol	213 ± 1	0.542	10.7
W-46-γ-Al_2O_3	Water	147 ± 1	0.414	9.1
ES-47-γ-Al_2O_3	Ethanolic solution	148 ± 1	0.367	11.3

Table 2. Textural properties of the of the W-46 and ES-47 composites.

Sample Support	S_{BET} (m^2/g)	Vp (cm^3/g)	Average Pore Size (nm)
W-46-LiCl	68 ± 1	0.196	8.7
W-46-$CaCl_2$	81 ± 1	0.252	8.3
ES-47-LiCl	96 ± 1	0.204	9.3
ES-47-$CaCl_2$	83 ± 1	0.207	10.2

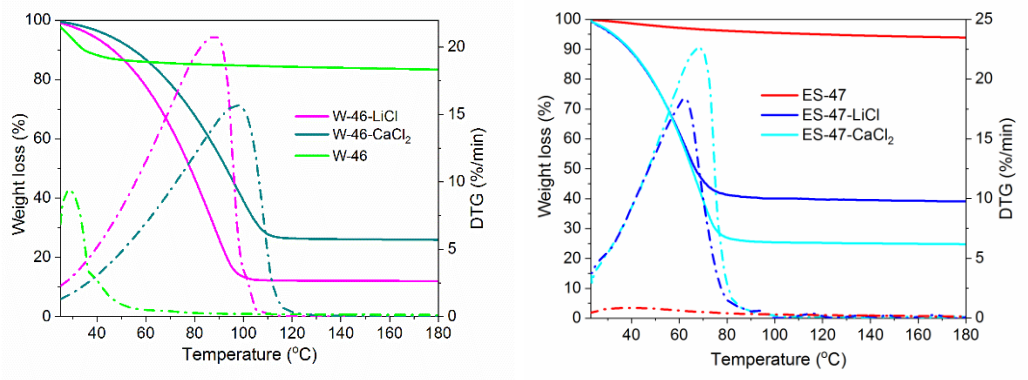

Figure 5. TG/DTG curves of the hydrothermally prepared support (**a**) W-46 and its composites and (**b**) ES-47 and its composites.

3.2. Water Sorption Properties

The mesoporous γ-Al_2O_3 and composites exhibit Type V water sorption isotherms (Figure 6a), measured at 35 °C. The γ-Al_2O_3 supports showed weak hydrophilic properties, which are also characteristic of mesoporous silica materials [8]. It was observed that the water uptake increased slowly up to 0.08 g/g at a relative pressure of 0.7. Thereafter, the water sorption capacity increased suddenly from 0.08 g/g to 0.31 g/g, which is due to the mechanism of capillary condensation and shows the active role of the supports. Jabbari-Hichri [21] reported that mesoporous alumina impregnated with 14 wt% $CaCl_2$ showed a water sorption capacity of 0.17 g/g. The composite W-46-LiCl (2.89 g/g) exhibited the highest maximal water sorption capacity of all composites, as determined from water sorption isotherms measured at 35 °C. The ES-47-LiCl sample showed the maximal water uptake of 1.00 g/g. Composites containing $CaCl_2$ showed lower maximal water sorption capacities: 0.76 g/g for W-46-$CaCl_2$ and 0.46 g/g for ES-47-$CaCl_2$. At a relative pressure of 0.4, the W-46 composite with 10 wt% $CaCl_2$, showed 4.5 times greater water uptake (4% versus 18%) than the support W-46 (not shown), while the composite with 15 wt% LiCl revealed 18 times greater water uptake than its support (4% versus 71%). It can be concluded that the presence of the salts in the γ-Al_2O_3 support increases the water sorption capacity of the composites, and the salt content affects the sorption performance of these composites. It should be emphasized that, among all the composites, only the composite W-46-$CaCl_2$ exhibits a water sorption isotherm without hysteresis loop (Figure 6a) up a relative pressure of 0.4, which may further improve the heat storage performance. Small

hysteresis is seen in W-46-LiCl, while both ES-47 composites show larger hysteresis of the water sorption isotherm (Figure 6a inset).

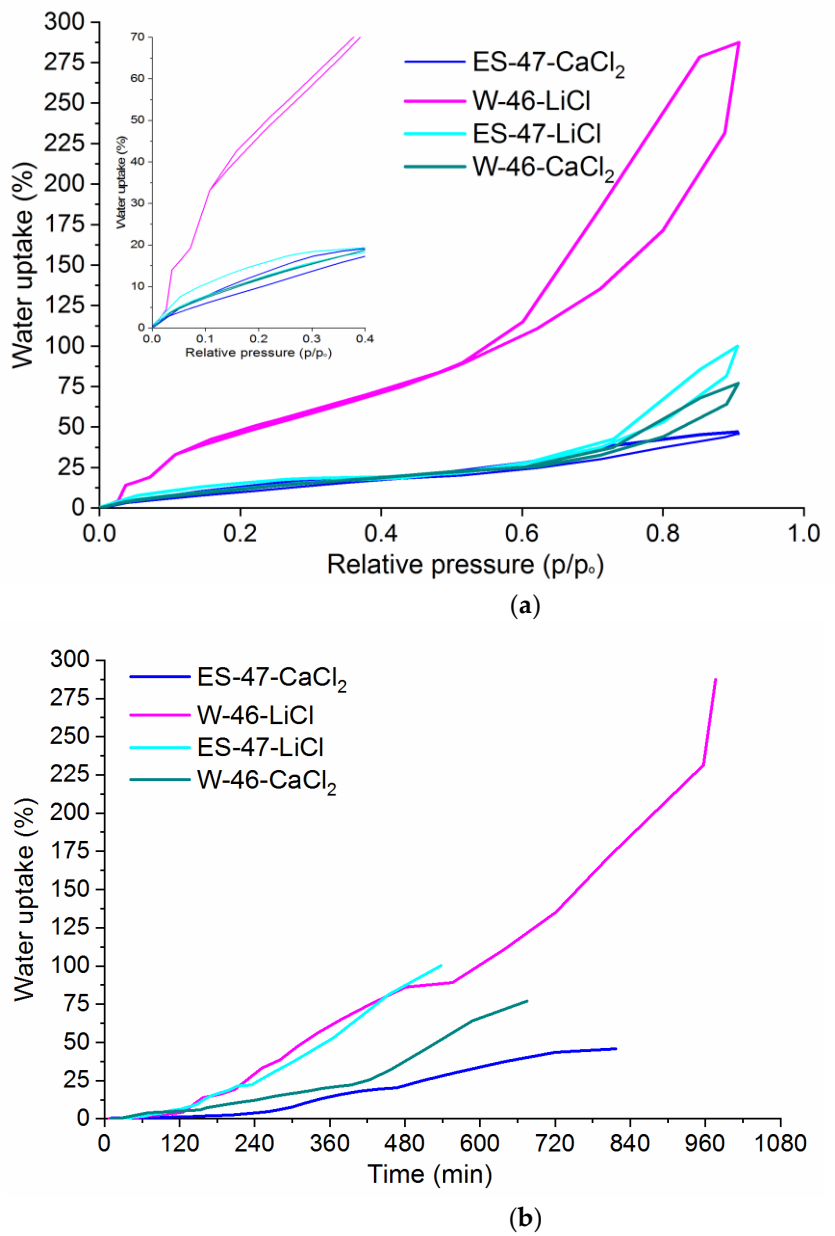

Figure 6. (**a**) Water uptake curves and (**b**) water sorption kinetics curves of the composites with W-46 and ES-47 supports at 35 °C.

The comparison of the water sorption isotherms of W-46-$CaCl_2$ and ES-47-$CaCl_2$ revealed differences in the range of $0 < p/p_0 < 0.4$, with the W-46-$CaCl_2$ sample showing slightly higher uptake, which is most likely due to the preparation procedure of the support in water. The water uptake at 0.4 relative pressure of the composite ES-47-$CaCl_2$, which has uniform mesopores with an average pore size of 10.2 nm and a total pore volume (0.207 cm^3/g), was 1.7% lower than the water uptake of the composite W-46-$CaCl_2$ with a smaller pore diameter (8.3 nm) and a larger total pore volume (0.252 cm^3/g). The water uptake curve of the composite with W-46-γ-Al_2O_3 and 15 wt% LiCl showed a plateau at 0.038 p/p_o due to the formation of lithium chloride hydrate [44], while this plateau was not observed for the composites with lower salt content.

The kinetic curves (Figure 6b) show that the maximal water uptake on the composite ES-47-LiCl was reached in the shortest time. The composite ES-47-$CaCl_2$ showed a slow

sorption rate in the first two hours, increasing with a slow rate after 2 h. The water sorption on the composites W-46-LiCl and ES-47-LiCl was also slow in the first two hours and then gradually increased at a higher rate than that of the composites containing $CaCl_2$. Water uptake occurred in the following order: ES-47-LiCl, W-46-$CaCl_2$, ES-47-$CaCl_2$, W-46-LiCl.

The integral heat of sorption is one of the most relevant parameters for evaluating the effectiveness of sorbent at the material level for TES. For sorption heat storage the adsorbents with high water loading lift between adsorption and desorption can reach high storage densities. The integral heat of sorption was calculated for the given boundary conditions for space heating [8]: sorption/condensation temperature of 30 °C, desorption temperature of 100 °C, and evaporation temperature of 10 °C. The integral heat of sorption Q_{sor} of all composites is listed in Table 3. Composites containing similar amounts of LiCl and $CaCl_2$ showed similar theoretical energy storage density values at material level ranging from 1.26 to 1.37 GJ/m^3, while lower values were obtained with composites containing mesoporous silica and the same amount of $CaCl_2$ [8].

Table 3. Water loading lift and the integral heat of adsorption for the composites.

Sample	Δw (kg/kg)	Q_{sor} (kWh/m^3)	Q_{sor} (GJ/m^3)
W-46-$CaCl_2$	0.127	350	1.26
W-46-LiCl	0.514	1437	5.17
ES-47-LiCl	0.137	380	1.37
ES-47-$CaCl_2$	0.135	377	1.36

The increased amount of the salt (15 wt% LiCl) in the composite increased the calculated water loading lifts, and consequently, theoretical energy storage density up to 5.17 GJ/m^3 at material level. The physical and structural properties of the mesoporous γ-Al_2O_3 support, such as high density and the suitable mesostructure with the pore size of up to 10 nm, are advantageous for the sorption heat storage performance, which can be further enhanced by the high thermal conductivity of the γ-alumina support. A direct comparison of the energy storage density of these composites with other alumina-containing composites was difficult, because it strongly depends on the boundary conditions. The value of energy storage density of the composite with LiCl (14.7 wt.%) and activated alumina prepared by wet impregnation equalled 1.14 GJ/m^3, considering a desorption temperature of 120 °C, sorption temperature of 20 °C, and 80% relative humidity [11]. This composite was also tested in the open sorption TES system for space heating at a desorption temperature of 110 °C and reached 0.69 GJ/m^3 [22]. The influence of different boundary conditions on the integral heat of sorption was evaluated (Figure 7) for the conditions of the space heating storage cycle defined in [1] for the Central European climate: sorption temperature of 35 °C, evaporation temperature of 5 °C, desorption temperature of 90 °C, and condensation temperature of 30 °C. Frazzica [1] used the condensation temperature of 30 °C as the average ambient temperature during the day in summer in Central Europe. The evaporation temperature was set at 5 °C, which was explained by the situation of some rigid climatic conditions where geothermal boreholes were used to provide ambient heat for the evaporator and satisfactory heat transfer inside the component.

It can be seen that lower desorption temperature decreases the energy storage density of the composites and still promotes their use for low-temperature thermal energy storage.

The cycling stability of the W-46-$CaCl_2$ (without hysteresis during the sorption cycle up to a relative pressure of 0.4) and W-46-LiCl (small hysteresis during the sorption cycle up to relative pressure of 0.4) composites was tested during 25 sorption and desorption cycles between 35 and 100 °C at 12 mbar, showing a small reduction in water uptake of 2.0% for W-46-$CaCl_2$ and 1.5% for W-46-LiCl after the last cycle (Figure 8). After the cycle tests, no salt leakage was observed for these samples. This confirms that the mesoporous γ-Al_2O_3 support can be used as a stable nano-environment for the entrapment of calcium

and lithium chloride. These composites are promising candidates for low-temperature thermal energy storage.

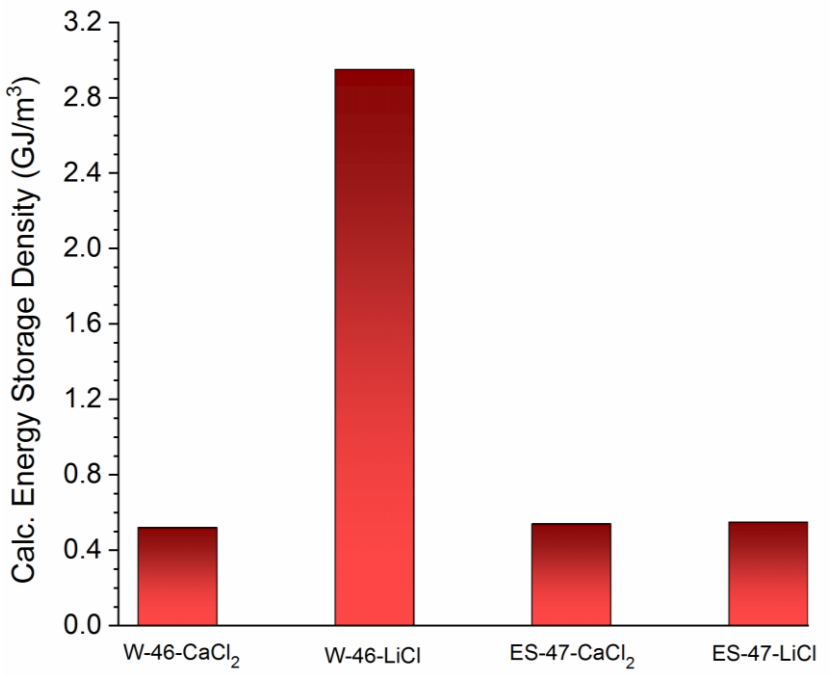

Figure 7. The integral heat of sorption of the composites for space heating storage cycle: sorption temperature of 35 °C, evaporation temperature of 5 °C, desorption temperature of 90 °C, and condensation temperature of 30 °C.

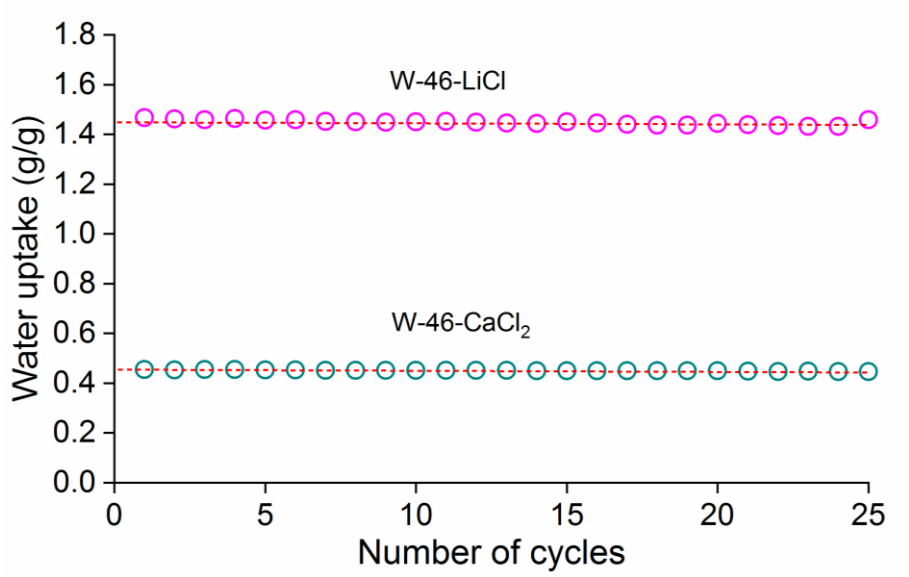

Figure 8. Cycling stability of 25 cycles of sorption and desorption for W-46-$CaCl_2$ and W-46-LiCl between 35 °C and 100 °C at 12.5 mbar.

4. Conclusions

Mesoporous γ-alumina supports were synthesized from gels containing aluminium isopropoxide, the surfactant Pluronic F-127, and various solvents: ethanol, water, or ethanolic solution. This was undertaken by the two-step synthesis procedure, which included the evaporation-induced self-assembly method followed by solvothermal or hydrothermal treatment at 160 °C for 12 h and calcination at 800 °C to obtain the crystalline phase of γ-Al_2O_3. The solvents affected the uniformity of the mesopores, the specific surface

area, and the morphology of the γ-Al_2O_3 supports. The highest degree of uniformity of mesopores and surface area was found in the sample E-37 prepared in etanol. The uniformity of the samples ranged from the E-37 (ethanol) and ES-47 (etanolic solution) to W-46 (water). The solvent also influenced the surface charge of the γ-Al_2O_3 support and, consequently, the amount of the salt inclusion in the support performed by incipient wetness impregnation. The desorption temperatures of all composites varied from 62 to 98 °C, indicating low temperature heat storage utilization.

Among all composites, the highest heat storage density (5.17 GJ/m^3) was achieved for W-46-LiCl at boundary conditions for space heating at the sorption and condensation temperature of 30 °C, the desorption temperature of 100 °C, and the evaporation temperature of 10 °C. The composite W-46-$CaCl_2$ showed the best heat storage performance in terms of fast kinetics of water sorption, no sorption–desorption hysteresis, low desorption temperature, and very good cycling stability and energy storage density of 1.26 GJ/m^3. The fastest rate of water sorption was found for ES-47-LiCl composite, where the sorption of water reached its maximum after 9 h. Moreover, after 25 cycles between 35 °C and 100 °C at 12.5 mbar, small decreases in water uptake of 1.5 and 2.0 % were observed for the W-46-$CaCl_2$ and W-46-LiCl composites, respectively, indicating the very good hydrothermal stability of these composites.

The properties of mesoporous γ-Al_2O_3 supports such as high density, particular mesostructure, high thermal conductivity, and structure stability are advantageous characteristics for the preparation and use of these TCM composites as low-temperature sorption heat storage materials. This study opens up several possibilities to tailor the porosity of mesostructured oxide supports by proper selection of solvents, reagents, and synthesis routes. Moreover, it represents an important step towards the development of mesostructured metal oxides with designed properties for TCM materials, which are of great importance for thermochemical energy storage.

Author Contributions: Conceptualization, A.R.; formal analysis, M.O., A.R.; investigation, M.O.; writing—original draft preparation, A.R.; writing—review and editing, N.Z.L.; visualization A.R.; supervision, A.R.; project administration, A.R.; funding acquisition, N.Z.L. All authors have read and agreed to the published version of the manuscript.

Funding: The Slovenian Research Agency is thanked for the support of the research program P1-0021 (Nanoporous materials).

Institutional Review Board Statement: Not applicable.

Informed Consent Statement: Not applicable.

Data Availability Statement: Not applicable.

Acknowledgments: We thank Suzana Mal for water sorption and nitrogen physisorption measurements, Andraž Krajnc for cycling stability test and Matjaž Mazaj for SEM pictures.

Conflicts of Interest: The authors declare no conflict of interest.

References

1. Frazzica, A.; Brancato, V.; Caprì, A.; Cannilla, C.; Gordeeva, L.G.; Aristov, Y.I. Development of "Salt in Porous Matrix" Composites Based on LiCl for Sorption Thermal Energy Storage. *Energy* **2020**, *208*, 118338. [CrossRef]
2. Gunasekara, S.N.; Barreneche, C.; Inés, A.; Díaz, A.C.; Ristić, A.; Weinberger, P.; Paksoy, H.Ö.; Koçak, B.; Rathgeber, C.; Chiu, N.; et al. Thermal Energy Storage Materials (TESMs)—What Does It Take to Make Them Fly ? *Crystals* **2021**, *11*, 1276. [CrossRef]
3. Gordeeva, L.G.; Aristov, Y.I. Composites "salt inside Porous Matrix" for Adsorption Heat Transformation: A Current State-of-the-Art and New Trends. *Int. J. Low-Carbon Technol.* **2012**, *7*, 288–302. [CrossRef]
4. Zbair, M.; Bennici, S. Survey Summary on Salts Hydrates and Composites Used in Thermochemical Sorption Heat Storage: A Review. *Energies* **2021**, *14*, 3105. [CrossRef]
5. Tokarev, M.; Gordeeva, L.; Romannikov, V.; Glaznev, I.; Aristov, Y. New Composite Sorbent $CaCl_2$ in Mesopores for Sorption Cooling/Heating. *Int. J. Therm. Sci.* **2002**, *41*, 470–474. [CrossRef]

6. Ristić, A.; Maučec, D.; Henninger, S.K.; Kaučič, V. New Two-Component Water Sorbent $CaCl_2$-$FeKIL_2$ for Solar Thermal Energy Storage. *Microporous Mesoporous Mater.* **2012**, *164*, 266–272. [CrossRef]
7. Silvester, L.; Touloumet, Q.; Kamaruddin, A.; Chassagneux, F.; Postole, G.; Auroux, A.; Bois, L. Influence of Silica Functionalization on Water Sorption and Thermochemical Heat Storage of Mesoporous SBA-15/$CaCl_2$ Composites. *ACS Appl. Energy Mater.* **2021**, *4*, 5944–5956. [CrossRef]
8. Ristić, A.; Zabukovec Logar, N. New Composite Water Sorbents $CaCl_2$-PHTS for Low-Temperature Sorption Heat Storage: Determination of Structural Properties. *Nanomaterials* **2018**, *9*, 27. [CrossRef] [PubMed]
9. Nonnen, T.; Beckert, S.; Gleichmann, K.; Brandt, A.; Unger, B.; Kerskes, H.; Mette, B.; Bonk, S.; Badenhop, T.; Salg, F.; et al. A Thermochemical Long-Term Heat Storage System Based on a Salt/Zeolite Composite. *Chem. Eng. Technol.* **2016**, *39*, 2427–2434. [CrossRef]
10. D'Ans, P.; Skrylnyk, O.; Hohenauer, W.; Courbon, E.; Malet, L.; Degrez, M.; Descy, G.; Frère, M. Humidity Dependence of Transport Properties of Composite Materials Used for Thermochemical Heat Storage and Thermal Transformer Appliances. *J. Energy Storage* **2018**, *18*, 160–170. [CrossRef]
11. Zhang, Y.N.; Wang, R.Z.; Li, T.X. Thermochemical Characterizations of High-Stable Activated Alumina/LiCl Composites with Multistage Sorption Process for Thermal Storage. *Energy* **2018**, *156*, 240–249. [CrossRef]
12. Brancato, V.; Gordeeva, L.G.; Caprì, A.; Grekova, A.D.; Frazzica, A. Experimental Comparison of Innovative Composite Sorbents for Space Heating and Domestic Hot Water Storage. *Crystals* **2021**, *11*, 476. [CrossRef]
13. Permyakova, A.; Wang, S.; Courbon, E.; Nouar, F.; Heymans, N.; D'Ans, P.; Barrier, N.; Billemont, P.; De Weireld, G.; Steunou, N.; et al. Design of Salt-Metal Organic Framework Composites for Seasonal Heat Storage Applications. *J. Mater. Chem. A* **2017**, *5*, 12889–12898. [CrossRef]
14. Calabrese, L.; Bonaccorsi, L.; Bruzzaniti, P.; Gullì, G.; Freni, A.; Proverbio, E. Zeolite Filled Siloxane Composite Foams: Compression Property. *J. Appl. Polym. Sci.* **2018**, *135*, 46145. [CrossRef]
15. Kallenberger, P.A.; Posern, K.; Linnow, K.; Brieler, F.J.; Steiger, M.; Fröba, M. Alginate-Derived Salt/Polymer Composites for Thermochemical Heat Storage. *Adv. Sustain. Syst.* **2018**, *2*, 1–8. [CrossRef]
16. Frazzica, A.; Brancato, V.; Dawoud, B. Unified Methodology to Identify the Potential Application of Seasonal Sorption Storage Technology. *Energies* **2020**, *13*, 1037. [CrossRef]
17. Wang, L.W.; Metcalf, S.J.; Critoph, R.E.; Tamainot-Telto, Z.; Thorpe, R. Two Types of Natural Graphite Host Matrix for Composite Activated Carbon Adsorbents. *Appl. Therm. Eng.* **2013**, *50*, 1652–1657.
18. Yan, T.; Li, T.; Xu, J.; Chao, J.; Wang, R.; Aristov, Y.I.; Gordeeva, L.G.; Dutta, P.; Murthy, S.S. Ultrahigh-Energy-Density Sorption Thermal Battery Enabled by Graphene Aerogel-Based Composite Sorbents for Thermal Energy Harvesting from Air. *ACS Energy Lett.* **2021**, *6*, 1795–1802. [CrossRef]
19. An, G.; Zhang, Y.; Wang, L.; Zhang, B. An Advanced Composite Sorbent with High Thermal Stability and Superior Sorption Capacity without Hysteresis for a Better Thermal Battery. *J. Mater. Chem. A* **2020**, *8*, 11849–11858. [CrossRef]
20. Dawoud, B.; Aristov, Y. Experimental Study on the Kinetics of Water Vapor Sorption on Selective Water Sorbents, Silica Gel and Alumina under Typical Operating Conditions of Sorption Heat Pumps. *Int. J. Heat Mass Transf.* **2003**, *46*, 273–281. [CrossRef]
21. Jabbari-Hichri, A.; Bennici, S.; Auroux, A. $CaCl_2$-Containing Composites as Thermochemical Heat Storage Materials. *Sol. Energy Mater. Sol. Cells* **2017**, *172*, 177–185. [CrossRef]
22. Zhang, Y.N.; Wang, R.Z.; Li, T.X. Experimental Investigation on an Open Sorption Thermal Storage System for Space Heating. *Energy* **2017**, *141*, 2421–2433. [CrossRef]
23. Xu, S.Z.; Wang, R.Z.; Wang, L.W.; Zhu, J. Performance Characterizations and Thermodynamic Analysis of Magnesium Sulfate-Impregnated Zeolite 13X and Activated Alumina Composite Sorbents for Thermal Energy Storage. *Energy* **2019**, *167*, 889–901. [CrossRef]
24. Wu, H.; Salles, F.; Zajac, J. A Critical Review of Solid Materials for Low-Temperature Thermochemical Storage of Solar Energy Based on Solid-Vapour Adsorption in View of Space Heating Uses. *Molecules* **2019**, *24*, 945. [CrossRef] [PubMed]
25. Grekova, A.D.; Girnik, I.S.; Nikulin, V.V.; Tokarev, M.M.; Gordeeva, L.G.; Aristov, Y.I. New Composite Sorbents of Water and Methanol "Salt in Anodic Alumina": Evaluation for Adsorption Heat Transformation. *Energy* **2016**, *106*, 231–239. [CrossRef]
26. Henninger, S.K.; Ernst, S.J.; Gordeeva, L.; Bendix, P.; Fröhlich, D.; Grekova, A.D.; Bonaccorsi, L.; Aristov, Y.; Jaenchen, J. New Materials for Adsorption Heat Transformation and Storage. *Renew. Energy* **2017**, *110*, 59–68. [CrossRef]
27. Afshar Taromi, A.; Kaliaguine, S. Synthesis of Ordered Mesoporous Γ-Alumina—Effects of Calcination Conditions and Polymeric Template Concentration. *Microporous Mesoporous Mater.* **2017**, *248*, 179–191. [CrossRef]
28. Trueba, M.; Trasatti, S.P. γ-Alumina as a Support for Catalysts: A Review of Fundamental Aspects. *Eur. J. Inorg. Chem.* **2005**, *2005*, 3393–3403. [CrossRef]
29. Xu, X.; Megarajan, S.K.; Zhang, Y.; Jiang, H. Ordered Mesoporous Alumina and Their Composites Based on Evaporation Induced Self-Assembly for Adsorption and Catalysis. *Chem. Mater.* **2020**, *32*, 3–26. [CrossRef]
30. Žilková, N.; Zukal, A.; Čejka, J. Synthesis of Organized Mesoporous Alumina Templated with Ionic Liquids. *Microporous Mesoporous Mater.* **2006**, *95*, 176–179. [CrossRef]
31. Grant, S.M.; Vinu, A.; Pikus, S.; Jaroniec, M. Adsorption and Structural Properties of Ordered Mesoporous Alumina Synthesized in the Presence of F127 Block Copolymer. *Colloids Surf. A: Physicochem. Eng. Asp.* **2011**, *385*, 121–125. [CrossRef]

32. Gonçalves, A.A.S.; Costa, M.J.F.; Zhang, L.; Ciesielczyk, F.; Jaroniec, M. One-Pot Synthesis of $MeAl_2O_4$ (Me = Ni, Co, or Cu) Supported on γ-Al_2O_3 with Ultralarge Mesopores: Enhancing Interfacial Defects in γ-Al_2O_3 to Facilitate the Formation of Spinel Structures at Lower Temperatures. *Chem. Mater.* **2018**, *30*, 436–446. [CrossRef]
33. Brunauer, S.; Emmett, P.H.; Teller, E. Adsorption of Gases in Multimolecular Layers. *J. Am. Chem. Soc.* **1938**, *60*, 309–319. [CrossRef]
34. Kruk, M.; Jaroniec, M.; Sayari, A. Application of Large Pore MCM-41 Molecular Sieves to Improve Pore Size Analysis Using Nitrogen Adsorption Measurements. *Langmuir* **1997**, *13*, 6267–6273. [CrossRef]
35. Jaroniec, M.; Solovyov, L.A. Improvement of the Kruk-Jaroniec-Sayari Method for Pore Size Analysis of Ordered Silicas with Cylindrical Mesopores. *Langmuir* **2006**, *22*, 6757–6760. [CrossRef]
36. Ristić, A.; Fischer, F.; Hauer, A.; Zabukovec Logar, N. Improved Performance of Binder-Free Zeolite y for Low-Temperature Sorption Heat Storage. *J. Mater. Chem. A* **2018**, *6*, 11521–11530. [CrossRef]
37. Nuhnen, A.; Janiak, C. A Practical Guide to Calculate the Isosteric Heat/Enthalpy of Adsorption: Via Adsorption Isotherms in Metal-Organic Frameworks, MOFs. *Dalton Trans.* **2020**, *49*, 10295–10307. [CrossRef] [PubMed]
38. Krajnc, A.; Varlec, J.; Mazaj, M.; Ristić, A.; Logar, N.Z.; Mali, G. Superior Performance of Microporous Aluminophosphate with LTA Topology in Solar-Energy Storage and Heat Reallocation. *Adv. Energy Mater.* **2017**, *7*, 1601815. [CrossRef]
39. Calvin, J.J.; Asplund, M.; Zhang, Y.; Huang, B.; Woodfield, B.F. Heat Capacity and Thermodynamic Functions of Γ-Al_2O_3. *J. Chem. Thermodyn.* **2017**, *112*, 77–85. [CrossRef]
40. Frazzica, A.; Brancato, V. Verification of Hydrothermal Stability of Adsorbent Materials for Thermal Energy Storage. *Int. J. Energy Res.* **2019**, *43*, 6161–6170. [CrossRef]
41. Šuligoj, A.; Ristić, A.; Dražić, G.; Pintar, A.; Logar, N.Z.; Tušar, N.N. Bimetal Cu-Mn Porous Silica-Supported Catalyst for Fenton-like Degradation of Organic Dyes in Wastewater at Neutral PH. *Catal. Today* **2020**, *358*, 270–277. [CrossRef]
42. Thommes, M.; Kaneko, K.; Neimark, A.V.; Olivier, J.P.; Rodriguez-Reinoso, F.; Rouquerol, J.; Sing, K.S.W. Physisorption of Gases, with Special Reference to the Evaluation of Surface Area and Pore Size Distribution (IUPAC Technical Report). *Pure Appl. Chem.* **2015**, *87*, 1051–1069. [CrossRef]
43. Tušar, N.N.; Ristić, A.; Mali, G.; Mazaj, M.; Arčon, I.; Arčon, D.; Kaučič, V.; Logar, N.Z. MnO x Nanoparticles Supported on a New Mesostructured Silicate with Textural Porosity. *Chem. A Eur. J.* **2010**, *16*, 5783–5793. [CrossRef] [PubMed]
44. Sun, Y.; Spieß, A.; Jansen, C.; Nuhnen, A.; Gökpinar, S.; Wiedey, R.; Ernst, S.J.; Janiak, C. Tunable LiCl@UiO-66 Composites for Water Sorption-Based Heat Transformation Applications. *J. Mater. Chem. A* **2020**, *8*, 13364–13375. [CrossRef]